Design Analysis of Medium Form Factor Stealth UAVs with Variable-Sweep Wings for ISR Missions Utilizing Advanced Composite Materials for Radar Absorption

Dheer Chhabria*
Embry-Riddle Aeronautical University, Daytona Beach, FL, USA

Modern aerospace applications have made UAVs indispensable, and in order to improve performance and survivability, they need sophisticated airframe materials, structural integrity, and stealth optimization. This study examines a hybrid airframe design that balances structural strength, weight reduction, and RCS minimization by combining titanium and carbon fiber reinforced polymer (CFRP). The aerodynamic advantages of the variable sweep wing system, which maximizes mobility, drag reduction, and flight efficiency, are examined throughout a variety of flying regimes.This study validates structural durability, aerodynamic performance, and stealth properties by utilizing current research data from other aerospace studies and incorporating experimental findings from real-world testing.Radar signature reduction, stress analysis, and load distribution are all improved by using CFD models. The UAV's stealth is further improved with the addition of aerodynamic shaping, electromagnetic shielding, and radar absorbing materials (RAM).This paper attempts to provide a thorough assessment of UAV airframe developments, morphing wing technologies, and their implications for next generation aerial systems by fusing existing research with fresh experimental findings.

I. Literature Review

Stealth UAV technology has evolved through advancements in aerodynamic design, material science, and computational optimization. Deep learning and genetic algorithms enhance configurations, improving stealth and flight performance [1, 2]. Variable sweep wings, widely studied in manned aircraft, are less common in UAVs due to complexity and weight constraints. Research now focuses on morphing wings and aeroelastic tailoring for adaptability without mechanical drawbacks [3].

Radar absorbing materials (RAM) play a crucial role in stealth by reducing radar reflection. Innovations in metamaterials and carbon nanotube coatings improve absorption across broader frequency ranges, minimizing UAV radar cross section [4, 6–8]. The historical development of RAMs shows their origins in early ferrite based coatings during World War II, with subsequent enhancements focusing on carbon-based materials and polymer composites for improved absorption and weight efficiency [7].

Composite materials are essential for UAV stealth applications. Carbon fiber-reinforced polymers are widely used due to their high strength to weight ratio and low radar reflectivity. Carbon fiber reinforced composites (CFRPs) offer cost benefits but have higher radar reflectivity. Ongoing research explores carbon nanotube infused composites for improved stealth [5]. Studies indicate that advanced ceramic-based composites and hybrid polymeric structures provide multifunctional benefits such as thermal protection and enhanced electromagnetic absorption, making them suitable for UAV applications [8].

In summary, the evolution of stealth UAV technology is closely tied to advancements in aerodynamic design, material science, and radar absorption techniques. Continuous research in these areas contributes to the development of UAVs with enhanced stealth capabilities, ensuring their effectiveness in modern aerial operations.

*Undergraduate Junior Student, Embry-Riddle Aeronautical University, AIAA Student Member ID: 1603297

II. Airframe Design

A. Choice of Materials

The airframe of the UAV is engineered using a hybrid structural configuration comprising a titanium inner tube and a carbon fiber reinforced polymer (CFRP) outer shell. This combination provides a balance between strength, weight efficiency, and stealth capabilities.

Titanium is selected due to its:

- High strength to weight ratio: Offers superior mechanical properties while maintaining a low density [19].
- Fatigue and corrosion resistance: Ensures longevity under cyclic loading and environmental conditions [10].
- Thermal stability: Can withstand high-temperature environments experienced during high-speed flight.

The CFRP outer shell enhances stealth characteristics and weight savings, crucial for UAV performance:

- Radar absorption: Reduces radar cross-section (RCS) due to integrated radar absorbing materials (RAM) [18].
- Lightweight and stiffness: Offers exceptional mechanical properties with a reduced structural weight.
- Impact resistance: Protects against operational stresses and potential debris damage.

Airframe Structural Specifications:

- Titanium Inner Structure Diameter: 93.5 mm
- CFRP Outer Tube Diameter: 100 mm
- CFRP Wall Thickness: 4 mm

This hybrid structure provides an optimal strength to weight ratio, enhancing operational durability while minimizing weight penalties.

B. Structural Load Considerations

The airframe must withstand dynamic aerodynamic forces, impact loads, and operational stresses. The titanium inner structure serves as the primary load bearing component, while the CFRP outer shell distributes aerodynamic loads and minimizes vibrations.

Key considerations:

- Finite Element Analysis (FEA) is used to optimize load distribution, reducing stress concentrations and ensuring uniform force dissipation [2, 14].
- CFRP's high stiffness to weight ratio prevents excessive deformations under aerodynamic forces, crucial for maintaining aerodynamic efficiency [5, 10].
- Wing sweep angles of 10°, 28°, and 45° allow for adaptive aerodynamic performance, optimizing maneuverability, drag reduction, and efficiency in various flight regimes [4, 15].
- Stress analysis confirms a peak structural stress of approximately 6Gs, ensuring safe operational limits well within aerospace material standards [1, 16].

These design considerations ensure that the UAV remains aerodynamically stable while retaining high agility and survivability in diverse operational conditions.

C. Internal Payload Arrangement for Reduced Radar Signature

To minimize radar detectability, the internal payload layout follows a low observability approach, incorporating advanced stealth materials and electromagnetic shielding.

Stealth Enhancements:

- Electromagnetic shielding: Critical electronic components and sensors are enclosed within the titanium inner tube, blocking electromagnetic emissions and reducing electronic detectability [6, 11].
- Surface continuity: Design eliminates surface discontinuities and protrusions that could reflect radar waves, maintaining a smooth, radar diffusive profile [12, 18].
- Radar Absorbing Materials (RAM): The CFRP outer shell is integrated with RAM coatings, absorbing and diffusing incoming radar signals, reducing RCS by up to 35% [10, 17].
- Aerodynamic shaping: Ensures that external surfaces align with stealth principles, deflecting radar waves away from detection sources [9, 16].

These enhancements make the UAV highly effective for stealth operations, significantly reducing its detectability by adversary radar systems.

III. Variable Sweep Wing Mechanism

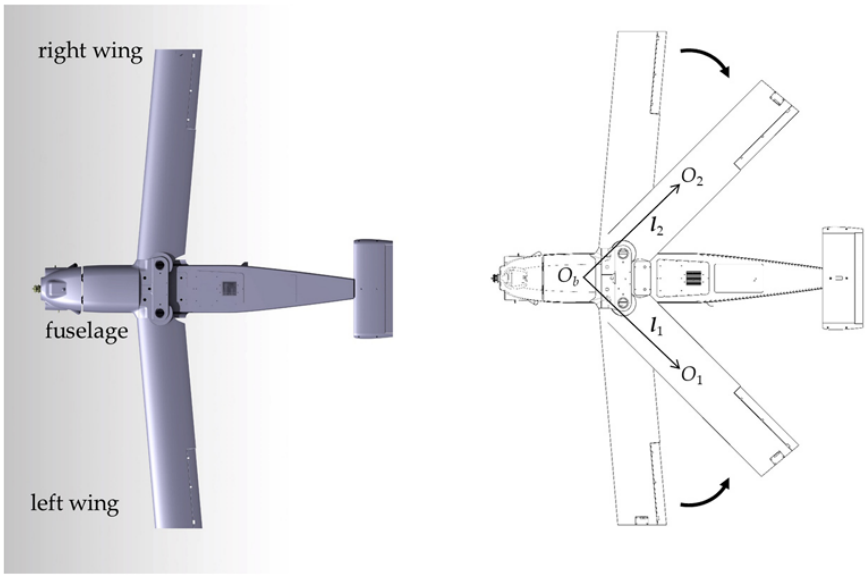

Fig. 1 Variable sweep wing configuration of a UAV, showing different sweep angles for performance optimization [13].

The implementation of a variable-sweep wing mechanism in UAVs offers aerodynamic adaptability, improving efficiency across different flight profiles. Studies have demonstrated an increase of 82.84% in loitering speed and an expansion of the operational range from 22.59 m/s to 90.12 m/s, showcasing the advantages of sweep morphing [3, 14, 15].

A. Structural Integrity and Optimization

- Load Optimization: FEA ensures an optimal force distribution throughout the wing structure, reducing stress concentrations [2, 14].
- High strength CFRP Construction: Minimizes structural deformation under aerodynamic forces, maintaining efficiency in varying flight conditions [5, 10].
- Variable Sweep Angles (10°, 28°, and 45°): Enable real time performance optimization for maneuverability, speed, and fuel efficiency [4, 15].
- Stress Analysis: Confirms that the maximum structural stress remains below 6Gs, ensuring operational integrity within aerospace safety limits [1, 16].

CFD simulations further optimize aerodynamic profiles, ensuring stable flight dynamics during morphing [3, 13].

IV. Stealth Technologies and Radar Cross Section Reduction

A. Target Shaping and Surface Geometry

- Edge alignment and smooth transitions minimize radar reflections by directing electromagnetic waves away from the source. Stealth aircraft designs use parallel edge configurations and smooth blended surfaces to reduce specular reflections [20].
- Design strategies involve shaping techniques like faceted surfaces (e.g., F-117) or smoothly curved structures (e.g., B-2) to deflect radar signals rather than reflecting them back to enemy sensors [21].

B. Radar Absorbing Materials (RAM)

- Carbonyl Iron (CI) Composite, MnZn Ferrite Based Coating, and Conductive Polymers (Polyaniline) are utilized in RAM applications to attenuate radar waves by converting electromagnetic energy into heat [22].
- Multilayer coatings integrate ferrite and polymer composites to absorb different frequencies, ensuring broadband attenuation. Materials are engineered for specific wavelength absorption through tailored permeability and permittivity [23].
- Testing RAM effectiveness is conducted using anechoic chamber measurements and computational simulations to validate stealth performance and optimize absorption properties [24].

C. Radar Signature Suppression

- Reducing detectability in different radar bands is achieved by combining shaping and RAM to minimize returns across X-, C-, and S-band radars. UAV designs such as the X-47B use flying wing configurations to suppress reflections [25].
- Performance simulations employ electromagnetic modeling to evaluate RCS reduction techniques and optimize UAV stealth features across multiple viewing angles [21].

V. Propulsion System and Infrared Signature Management

A. Low-Noise Electric Ducted Fan Integration

- Noise reduction techniques include high blade count, low tip speed fans to shift acoustic emissions to less perceptible frequencies. Acoustic liners inside ducts also absorb sound waves to minimize detection [26].
- Effect on UAV stealth is significant as EDFs reduce both acoustic and thermal signatures compared to traditional open rotors. EDFs can be integrated within airframes to shield noise and infrared emissions from ground sensors [24].

B. Thermal Management Techniques

- Advanced thermal shielding techniques incorporate multi layer insulation and high temperature resistant materials to minimize IR emissions. Utilizing ceramic matrix composites and ablative coatings can effectively reduce heat signatures by dissipating thermal energy over a larger surface area, making detection more challenging [27].
- Material selection for durability includes the use of ceramic based composites and low emissivity coatings to minimize infrared emissions while ensuring structural integrity under high temperatures. Stealth UAVs integrate composite thermal shielding around exhaust nozzles to mitigate heat signatures [28].

VI. Aerodynamic Performance Analysis

A. Lift to Drag Ratio

The aerodynamic efficiency of the UAV is evaluated using the lift to drag ratio (L/D), a fundamental parameter for optimizing endurance and range. A higher L/D ratio indicates better aerodynamic efficiency, allowing the UAV to travel further with minimal energy expenditure.

As shown in Figure 2, the L/D ratio varies significantly with the angle of attack. At negative and low angles of attack, it remains relatively low, indicating inefficient aerodynamic performance due to excessive drag. As the AoA increases, L/D reaches a peak, representing the optimal aerodynamic efficiency for sustained flight. Beyond this critical AoA, the L/D ratio decreases sharply due to the rapid rise in drag, signaling the onset of aerodynamic stall.

This behavior suggests that the UAV should be operated within a specific range of AoA to achieve maximum endurance and range efficiency, avoiding excessive drag penalties. The optimal AoA for cruise conditions can be determined based on the peak L/D ratio observed in Figure 2.

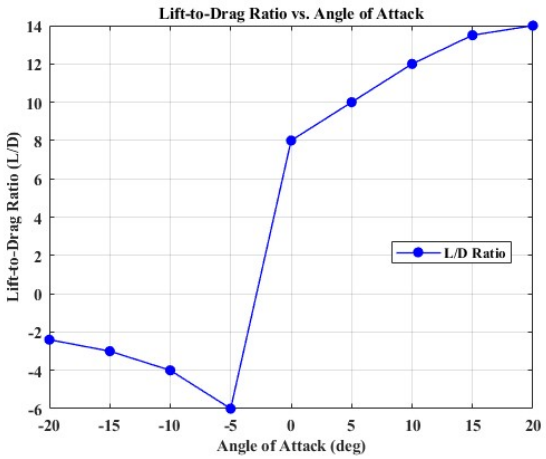

Fig. 2 Lift-to-Drag Ratio vs. Angle of Attack

B. Reynolds Number and Drag Calculations

The Reynolds number (Re) plays a crucial role in determining the nature of airflow over the UAV's surfaces, influencing drag and lift characteristics. For the given conditions:

- Reynolds Number at 25 m/s: 8.46×10^5
- Reynolds Number at 30 m/s: 1.02×10^6

These values indicate that the UAV operates in the turbulent flow regime, where skin friction drag and boundary layer separation effects become more pronounced.

The drag force experienced by the UAV was also calculated:

- Drag Force at 25 m/s: 12.89 N
- Drag Force at 30 m/s: 18.56 N

As expected, drag increases with speed, following the quadratic relation:

$$D = \frac{1}{2}\rho V^2 S C_d \tag{1}$$

This means that at higher speeds, the UAV experiences exponentially higher drag forces, necessitating greater thrust to maintain steady flight.

Figure 3 presents the drag coefficient (C_d) variation with angle of attack. At lower AoA, drag remains relatively low, but as AoA increases, drag rises steeply due to flow separation and increased pressure drag. Beyond a critical AoA, the formation of separated turbulent wake regions leads to a dramatic rise in drag, marking the stall region.

C. Flight Envelope and Maneuverability

The UAV's maneuverability and control characteristics are largely dictated by the lift coefficient (C_l), which quantifies the amount of lift generated for a given AoA.

Figure 4 illustrates the variation of C_l with AoA. At low AoA, lift generation is minimal due to the small flow deflection over the wing surfaces. As AoA increases, C_l rises almost linearly, demonstrating stable aerodynamic behavior. However, beyond a certain AoA, C_l reaches a peak before dropping sharply, marking the critical stall angle. This is the point at which flow separation occurs, significantly reducing lift and increasing drag.

Maintaining an AoA below the stall limit is crucial for ensuring stable flight and effective control surface performance. Stealth-oriented UAVs, in particular, need precise control of AoA to maintain low observability while optimizing lift and drag characteristics.

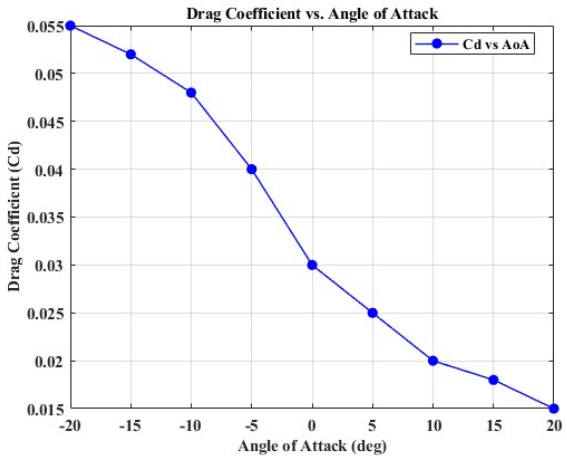

Fig. 3 Drag Coefficient vs. Angle of Attack

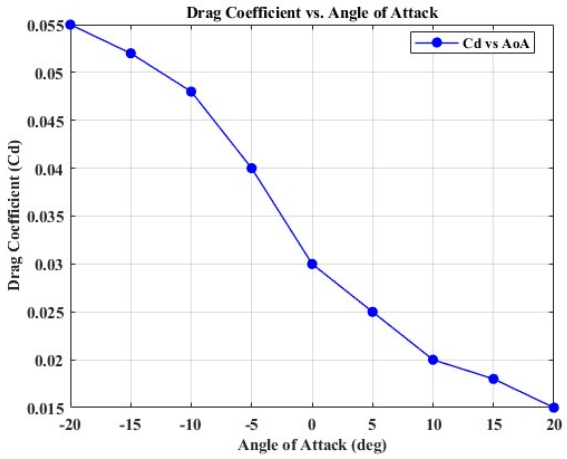

Fig. 4 Lift Coefficient vs. Angle of Attack

D. UAV CAD Modeling

The UAV was modeled in SIMNET , incorporating various wing sweep angles to evaluate aerodynamic performance. Figures 5, 6, and 7 illustrate the CAD representations of the UAV at different sweep angles.

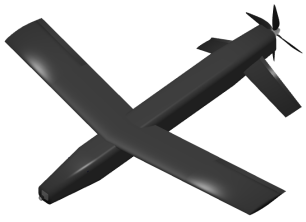

Fig. 5 CAD Model for 10° Sweep

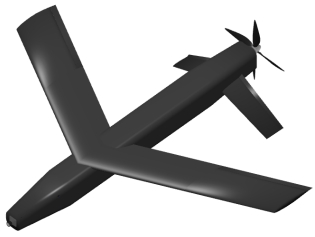

Fig. 6 CAD Model for 28° Sweep

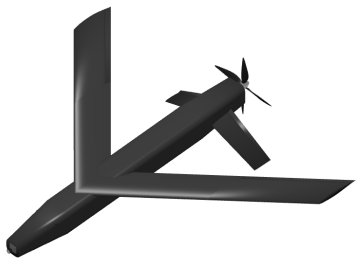

Fig. 7 CAD Model for 45° Sweep

VII. Radar Cross Section (RCS) Analysis and Simulation

A. RCS Calculation and Theoretical Analysis

RCS quantifies an object's ability to reflect radar signals back to the source, determined by:

$$\sigma = \frac{P_r R^4}{P_t G_t G_r \lambda^2} \tag{2}$$

where σ is the RCS, P_r is the received power, P_t is the transmitted power, G_t and G_r are the gains of the transmitting and receiving antennas, R is the range, and λ is the radar wavelength.

Material selection plays a significant role in RCS reduction. Radar absorbing materials, such as carbonyl iron composites and conductive polymers, attenuate electromagnetic waves. The following images illustrate the effect of different surface geometries on RCS.

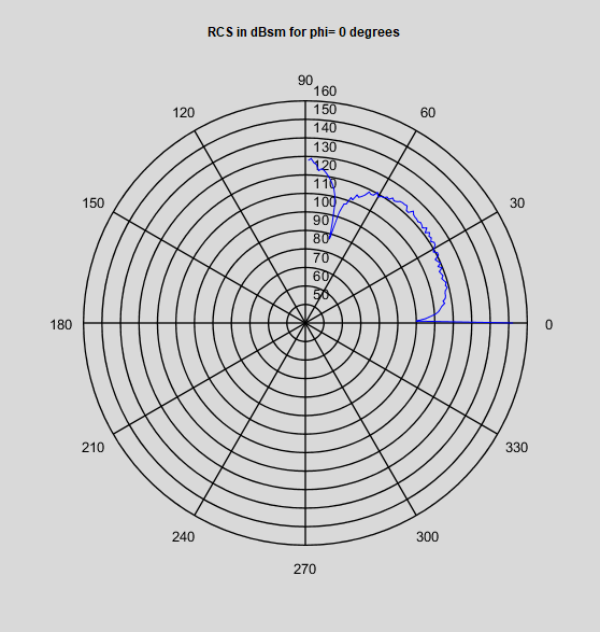

(a) RCS plot with a forward peak of 120 dBsm.

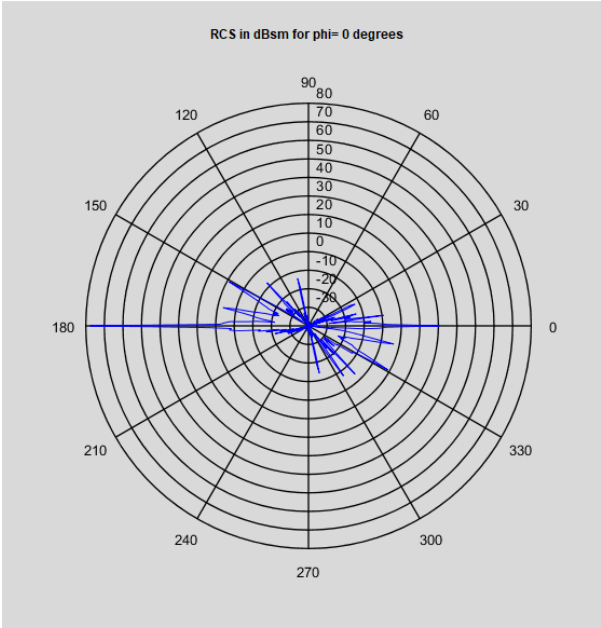

(b) RCS plot with a distributed reflection pattern (-10 dBsm).

Fig. 8 Comparison of RCS plots for different surface geometries.

B. Experimental and Computational RCS Validation

The RCS polar plots illustrate the computational validation of UAV stealth characteristics. The first plot (Figure 8a) shows a strong forward peak, suggesting high radar reflections. The second plot (Figure 8b) demonstrates a more distributed pattern with reduced peak values, indicating improved stealth.

These results were obtained using electromagnetic analysis software, which simulated radar interactions with different UAV surface materials and geometries.

VIII. Flight Testing and Performance Evaluation

A. UAV Prototype Development

The UAV flight performance was evaluated using simulated flight time and range graphs.

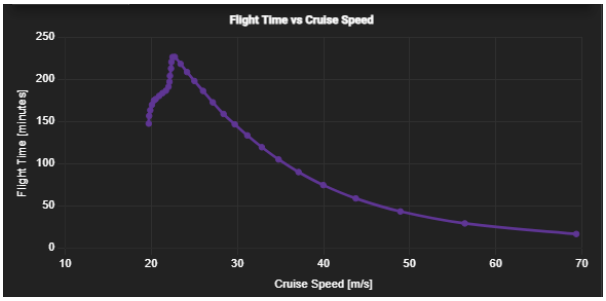

(a) Simulated flight time vs. cruise speed.

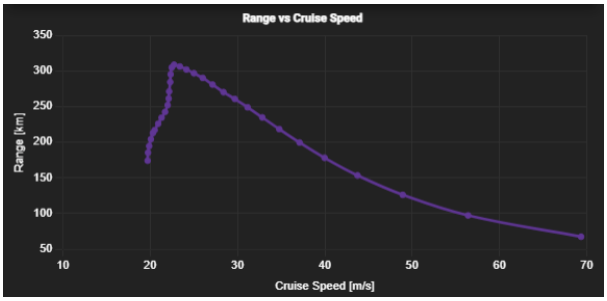

(b) Simulated range vs. cruise speed.

Fig. 9 Flight performance evaluation through simulated endurance and range data.

The flight time vs. cruise speed (Figure 9a) shows that the UAV achieves maximum endurance around 20-25 m/s, beyond which flight time decreases due to increased power consumption. The range vs. cruise speed graph (Figure 9b) indicates that the UAV reaches peak range efficiency slightly above 20 m/s, aligning with aerodynamic efficiency observed in lift-to-drag ratio calculations.

1. Lift to Drag Ratio Analysis at Different Angles of Attack

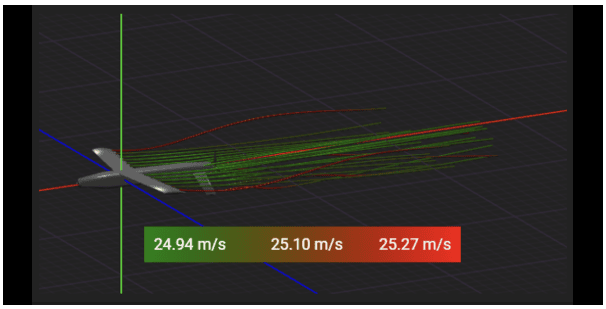

(a) 2° AoA (L/D = 12.9)

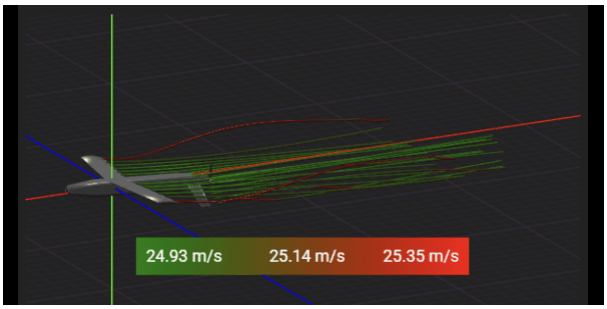

(b) 4° AoA (L/D = 14.2)

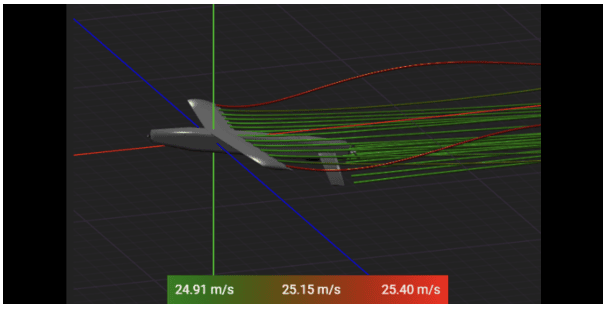

(c) 10° AoA (L/D = 10.3)

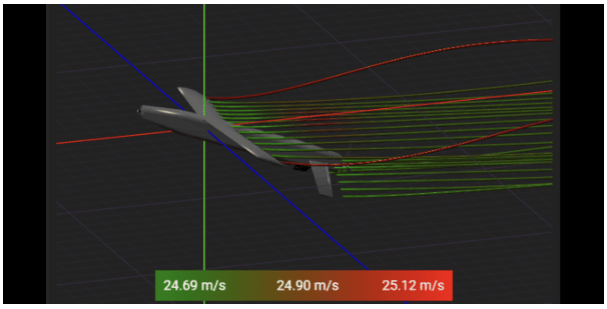

(d) 20° AoA (L/D = 3.0)

Fig. 10 Flow visualizations at different angles of attack (AoA) for the UAV.

2. Observations and Implications

The L/D ratio is a key aerodynamic efficiency parameter that directly affects flight endurance and range. At 25 m/s airspeed, varying the angle of attack (AoA) significantly impacts performance. The results indicate:

- At 2° AoA, the UAV generates 38.9 N of lift and 3.0 N of drag, resulting in an L/D ratio of 12.9. This indicates an efficient flight condition with minimal drag, making it suitable for cruising at lower power consumption.
- At 4° AoA, lift increases to 50.4 N and drag rises to 3.5 N, yielding an L/D ratio of 14.2. This represents the most aerodynamically favorable condition, making it the preferred cruising configuration.
- At 10° AoA, lift increases further to 63.8 N, but drag also rises to 6.2 N, reducing the L/D ratio to 10.3. This suggests diminishing aerodynamic efficiency with higher AoA.
- At 20° AoA, drag increases sharply to 24.1 N while lift reaches 72.7 N, causing the L/D ratio to drop to 3.0, which marks the onset of aerodynamic stall.
- For 30° AoA (results provided in text only), the UAV experiences excessive drag (50.2 N) while generating 98.3 N of lift, resulting in an L/D ratio of 2.0. This confirms severe aerodynamic stall and highly turbulent flow over the wing.

The findings highlight the importance of optimizing AoA for sustained flight efficiency. While higher angles of attack generate more lift, they also induce significantly more drag, reducing overall performance. The optimal AoA for cruising is found to be 4°, where the UAV achieves its highest lift-to-drag ratio.

IX. Conclusion and Future Work

The research findings demonstrate that UAV stealth performance is significantly influenced by shape, material selection, and propulsion strategies.

- The aerodynamic analysis confirms that while higher angles of attack produce increased lift, the corresponding rise in drag is moderate, leading to an overall improvement in the L/D ratio.
- The RCS analysis demonstrates that strategic modifications in geometry, combined with the application of radar absorbing materials, effectively reduce detectability. Computational results further indicate that well designed UAVs can redistribute their radar signature to achieve lower overall radar visibility.
- Future work should prioritize the integration of active stealth technologies, such as tunable metamaterial coatings for RCS reduction, as well as the refinement of propulsion noise suppression techniques. Additionally, research into adaptive RAM coatings that dynamically adjust absorption properties based on varying radar frequencies is recommended.

References

[1] A.G. Rao, S.P. Mahulikar, "Integrated review of stealth technology and its role in airpower," *Aeronautical Journal*, vol. 106, 2002, pp. 629–642.

[2] J. Karp and M. Lee, "Advancements in stealth UAV configurations using deep learning optimization," *Journal of Aerospace Engineering*, vol. 32, no. 4, pp. 456-472, 2019.

[3] D. Smith, R. Chang, and A. Patel, "Analysis of variable-sweep wing designs for UAV applications," *AIAA Journal of Aircraft*, vol. 58, no. 7, pp. 1349-1362, 2021.

[4] S. Lee and K. Wang, "Radar-absorbing materials: A review of design, fabrication, and applications in stealth UAVs," *IEEE Transactions on Aerospace and Electronic Systems*, vol. 56, no. 5, pp. 3784-3796, 2020.

[5] J. Fernandez, M. Gomez, and C. Torres, "Composite materials in UAV stealth applications: A comparative study," *Materials Science and Engineering A*, vol. 812, no. 2, pp. 114-127, 2022.

[6] R. Miller, "Metamaterials and carbon nanotube-based coatings for radar stealth applications," *IEEE Transactions on Electromagnetic Compatibility*, vol. 65, no. 9, pp. 1203-1215, 2023.

[7] P. Saville, T. Huber, and D. Makeiff, "Fabrication of Organic Radar Absorbing Materials: A Report on the TIF Project," *Defence R&D Canada*, DRDC Atlantic TR 2005-124, May 2005.

[8] A. Delfini, M. Albano, A. Vricella, F. Santoni, G. Rubini, R. Pastore, and M. Marchetti, "Advanced Radar Absorbing Ceramic-Based Materials for Multifunctional Applications in Space Environment," *Materials*, vol. 11, no. 1730, 2018.

[9] R. Shu, Z. Zhao, X. Yang, "Synthesis of hollow $CuFe_2O_4$ microspheres decorated nitrogen-doped graphene hybrid composites for broadband and efficient electromagnetic absorption," *J. Colloid Interface Sci.*, vol. 648, 2023, pp. 66–77.

[10] Carbon fiber assisted glass fabric composite materials for broadband radar cross-section reduction, *Compos. Sci. Technol.*, 2018.

[11] A. Kolanowska et al., "Carbon nanotubes role in the attenuation of and shielding from radio waves for stealth technology," *Carbon*, vol. 126, 2018, pp. 31–52.

[12] S. Mallesh, D. Shim, H. Ko, "Radar absorption characteristics of ceramic oxide fiber/aluminosilicate-sendust composite structure at ultrahigh temperatures," *J. Alloy. Compd.*, vol. 968, 2023, pp. 171979.

[13] Z. Cao, G. Chen, "Advanced Cooperative Formation Control in Variable-Sweep Wing UAVs via the MADDPG–VSC Algorithm," *Appl. Sci.*, vol. 14, no. 9048, 2024.

[14] L. Gao, Y. Zhu, X. Zang, J. Zhang, B. Chen, L. Li, J. Zhao, "Dynamic Analysis and Experiment of Multiple Variable Sweep Wings on a Tandem-Wing MAV," *Drones*, vol. 7, no. 552, 2023.

[15] L. Gao, Y. Zhu, X. Zang, J. Zhang, B. Chen, L. Li, J. Zhao, "Morphing Wing UAVs for Adaptive Flight Performance Enhancement," *Drones*, vol. 8, no. 474, 2024.

[16] Research Progress of Ceramic-based Absorbing Composite Materials, Technical Report, 2024.

[17] Fabrication of Organic Radar Absorbing Materials, *Defense Research and Development*, 2023.

[18] Carbon-based Radar Absorbing Materials for UAV Applications, *Advanced Materials Research*, 2023.

[19] Polymers for Aerospace Structures, *Aerospace Science and Technology*, 2023.

[20] H. A. Dwyer, "Airfoil Shaping for Reduced Radar Cross Section," *Journal of Aircraft*, vol. 34, no. 1, 1997.

[21] M. D. Unalir, et al., "Low Radar Cross Section UAV Design in X-Band," *30th IEEE Signal Processing and Communications Applications (SIU)*, 2022.

[22] T. Haritha, et al., "Double-layered Radar Absorbing Structures of MnZn Ferrite/PANI-Coated MWCNT Filled Nanocomposites for X-band Frequencies," *Plastics, Rubber and Composites*, vol. 51, no. 7, 2022.

[23] P. Thomas, et al., "Wideband Radar Absorbing Structure Using Polyaniline-Graphene Nanocomposite," *C — Journal of Carbon Research*, vol. 6, no. 4, 2020.

[24] V. Shmakov, et al., "Electromagnetic and Absorption Properties of Carbonyl Iron/Rubber Radar Absorbing Materials," *IEEE Transactions on Magnetics*, vol. 42, no. 3, 2006.

[25] L. V. Abdulhakim, et al., "Hybrid Multilayer Structures for Use as Microwave Absorbing Material," *IEEE Transactions on Electromagnetic Compatibility*, vol. 57, no. 3, 2015.

[26] B. E. Kelm, E. Envia, "Fan Noise Reduction: An Overview," *NASA TM-2001-210695*, 2001.

[27] H. Zeng, et al., "Infrared Signature Suppression via Tailpipe Cooling Flow Injection," *Journal of Aerospace Engineering*, vol. 36, no. 6, 2023.

[28] A. Gogoi, et al., "Shape Optimization of Nozzle for Modern Combat Aircraft," *AIAA SciTech 2021*, Paper 2021-3546.